Functional characterization of a mouse testicular olfactory receptor and its role in chemosensing and in regulation of sperm motility

Nanaho Fukuda[1], Kentaro Yomogida[2], Masaru Okabe[2,3] and Kazushige Touhara[1,*]

[1]Department of Integrated Biosciences, The University of Tokyo, Chiba 277-8562, Japan
[2]Research Institute for Microbial Diseases, Osaka University, Osaka 565-0871, Japan
[3]Genome Information Research Center, Osaka University, Osaka 565-0871, Japan
*Author for correspondence (e-mail: touhara@k.u-tokyo.ac.jp)

Accepted 23 August 2004
Journal of Cell Science 117, 5835-5845 Published by The Company of Biologists 2004
doi:10.1242/jcs.01507

Summary

Although a subset of the olfactory receptor (OR) gene family is expressed in testis, neither their developmental profile nor their physiological functions have been fully characterized. Here, we show that MOR23 (a mouse OR expressed in the olfactory epithelium and testis) functions as a chemosensing receptor in mouse germ cells. In situ hybridization showed that MOR23 was expressed in round spermatids during stages VI-VIII of spermatogenesis. Lyral, a cognate ligand of MOR23, caused an increase in intracellular Ca^{2+} in a fraction of spermatogenic cells and spermatozoa. We also generated transgenic mice that express high levels of MOR23 in the testis and examined the response of their germ cells to lyral. The results provided evidence that lyral-induced Ca^{2+} increases were indeed mediated by MOR23. In a sperm accumulation assay, spermatozoa migrated towards an increasing gradient of lyral. Tracking and sperm flagellar analyses suggest that Ca^{2+} increases caused by MOR23 activation lead to modulation of flagellar configuration, resulting in chemotaxis. By contrast, a gradient of a cAMP analog or K8.6 solution, which elicit Ca^{2+} influx in spermatozoa, did not cause sperm accumulation, indicating that chemosensing and regulation of sperm motility was due to an OR-mediated local Ca^{2+} increase. The present studies indicate that mouse testicular ORs might play a role in chemoreception during sperm-egg communication and thereby regulate fertilization.

Key words: Chemotaxis, Calcium, Olfactory receptor, Testis, Sperm, Odorant

Introduction

The G-protein-coupled olfactory receptors (ORs) make up a large multigene family that includes approximately 1000 members in mice (Zhang and Firestein, 2002). Functional characterization of ORs has shown that they recognize a wide range of odorants in the olfactory epithelium (Firestein, 2001; Mombaerts, 1999; Touhara, 2002) and that a combination of activated ORs encodes the identities of different odorants (Kajiya et al., 2001; Malnic et al., 1999; Touhara, 2001). Interestingly, some genes belonging to the OR family are expressed in the male germ cells of mammals, including human, dog, rat and mouse (Parmentier et al., 1992; Vanderhaeghen et al., 1997). In these cases, the OR proteins appear to be expressed in late spermatids and on the tail midpiece of mature spermatozoa, implying that testicular ORs are involved in sperm maturation, migration or fertilization (Vanderhaeghen et al., 1993; Walensky et al., 1995).

In olfactory neurons, odorants bind to ORs, which activate G proteins and initiate signal transduction via adenylyl cyclase. This leads to the opening of cyclic-nucleotide-gated (CNG) channels and Ca^{2+} influx (Firestein, 2001). Some of the components in the olfactory pathways, such as $G\alpha_{olf}$, adenylyl cyclase III and CNG channels, are also expressed in testis and sperm (Defer et al., 1998; Gautier-Courteille et al., 1998; Weyand et al., 1994; Wiesner et al., 1998), suggesting that testicular ORs can recruit the same cAMP-Ca^{2+} signaling cascade as in the olfactory epithelium. This concept is also supported by the finding that β-arrestin2, which might mediate the desensitization of ORs, is localized with OR proteins in the mid-piece of rat sperm (Dawson et al., 1993; Walensky et al., 1995).

Ca^{2+} and cyclic nucleotides are also key elements in the regulation of sperm motility in many species. For example, resact, a chemoattractant peptide from the sea urchin (Ward et al., 1985), binds to a membrane receptor on sperm and increases cGMP levels, followed by a transient influx of Ca^{2+} (Kaupp et al., 2003; Kirkman-Brown et al., 2003). Sperm-activating and -attracting factor from ascidian sperm, which was recently identified as a sulfated steroid (Yoshida et al., 2002), also causes Ca^{2+} influx and an increase in intracellular cAMP in sperm (Izumi et al., 1999). Furthermore, many studies in mammals have demonstrated an association between sperm motility and increased intracellular Ca^{2+} and/or cAMP levels (Baldi et al., 2002; Darszon et al., 2001; Suarez and Ho, 2003). Collectively, these observations suggest that cyclic nucleotides and Ca^{2+} play an important role in the regulation of sperm motility.

Given this evidence, it is conceivable that testicular ORs

function as chemotactic receptors in sperm via the cAMP-Ca^{2+}-CNG channel-signaling cascade. Indeed, bourgeonal (a ligand for human OR17-4) was recently shown to cause an increase in intracellular Ca^{2+} as well as chemotaxis in human sperm (Spehr et al., 2003). Although bourgeonal is probably not an endogenous compound in the body, the study supported the idea that human ORs act as chemoreceptors for small molecules in sperm.

In addition, MOR23 [a mouse OR encoded by the *MOR267-13* (Olfr16) gene] is expressed in the olfactory epithelium as well as in the testis (Asai et al., 1996). MOR23 was functionally cloned from single olfactory neurons that responded to the floral odorant lyral (Touhara et al., 1999). The response was recapitulated in both homologous and heterologous expression systems, verifying that one of the cognate ligands for MOR23 is lyral (Touhara et al., 1999). Because MOR23 appears to function as a receptor for lyral in the olfactory epithelium, it is possible that MOR23 acts as a chemoreceptor in the testis. To clarify the function of testicular ORs in mice, we analysed the developmental expression of MOR23 in testis and the responsiveness of germ cells to lyral. Furthermore, we generated transgenic (Tg) mice that express high levels of MOR23 in testis to clarify its functional role in sperm. Herein, we demonstrate that MOR23 is functionally expressed in mouse spermatogenic cells and sperm, and that MOR23 activation increases intracellular Ca^{2+} and regulates sperm motility.

Materials and Methods

Odorants and reagents

Odorants used in this study were kindly provided by T. Hasegawa. Purities of odorants were checked by thin-layer chromatography before use. Odorant solutions were directly suspended by sonication in the buffer used in each assay to make 5 mM (for Ca^{2+} imaging of HEK 293 cells and spermatogenic cells) or 50 mM (for Ca^{2+} imaging of spermatozoa) stock solution and diluted to the indicated concentrations before the experiments. 8-Br-cAMP was purchased from Calbiochem (CA, USA).

RT-PCR analysis

Total RNA was prepared from tissues of adult C57BL/6CrSlc mice (Japan SLC, Hamamatsu, Japan) using TRIzol reagent (Life Technologies). DNase-I-treated RNA was reverse-transcribed using Superscript II (Life Technologies) and *Not*I-$(dT)_{18}$ primer (Pharmacia Biotech). 1/20th of the reverse-transcribed mixture was subjected to polymerase chain reaction (PCR) with 5′ primer specific for the MOR23-encoding gene and 3′ *Not*I primer. Nested PCR was performed with 1/50th of first PCR products and primers specific for MOR23. Amplifications were carried out for 35 cycles (94°C for 30 seconds, 55°C for 30 seconds, 72°C for 1 minute).

In situ hybridization

Digoxigenin (DIG)-labeled sense and antisense probes were prepared from full-length MOR23, protamine 1 and H1t coding sequences in pBluescript II SK (+) (Stratagene) using DIG RNA labeling mix (Roche). 10-15-week-old C57BL/6CrSlc mice were sacrificed by cervical dislocation and perfused intracardially with 4% paraformaldehyde (PFA) in PBS. The testes were rapidly embedded in OCT (optimal cutting temperature compound) (Sakura, Tokyo, Japan) and cryostat sections (20 μm) were mounted on a Matsunami Adhesive Slide-coated glass slide (Mastunami Glass IND., Japan). Serial sections were used to compare the expression patterns of different genes. Slides were postfixed with 4% PFA in PBS, treated with 0.3% H_2O_2 in PBS, acetylated and then incubated overnight at 65°C with 200 μl hybridization buffer (50% formamide, 10 mM Tris-HCl, pH 7.0, 0.2 ng ml^{-1} tRNA, 10% dextran sulfate, 1× Denhardt's solution, 600 mM NaCl, 0.25% sodium-dodecyl-sulfate (SDS), 5 mM EDTA) containing 50 ng DIG-labeled probe. The sections were washed at 65°C successively with 50% formamide in 2× SSC, 2× SSC and 0.2× SSC. Hybridization signals were detected using a tyramid signal amplification (TSA) biotin system (PerkinElmer Life Science) according to the manufacturer's protocol. Briefly, sections were blocked with 0.5% blocking reagent and incubated with sheep horseradish peroxidase (HRP)-conjugated anti-DIG Fab fragment (Roche). Signals were amplified by incubating the sections with biotinyl-tyramide and with alkaline phosphatase (AP) or HRP-conjugated streptavidin. The sections were then incubated with NBT/BCIP (nitroblue tetrazolium chloride / 5-bromo-4-chloro-3-indolyl-phosphate, toluidine salt) (Roche) to detect bound streptavidin-AP or with DAB (3,3′-diaminobenzidene) (Sigma-Aldrich) for bound streptavidin-HRP. Finally, the sections stained with DAB were counterstained with methyl green (DAKO).

Construction of Tg mice expressing MOR23 in the testes

A Flag-tagged MOR23-encoding gene was introduced into pBluescript II SK (–) downstream of the calmegin promoter sequence (Watanabe et al., 1995) and upstream of the rabbit poly-A attachment sequence. The construct was excised with *Sal*I and *Hin*dIII, separated by agarose gel electrophoresis and purified using a Qiaquick gel extraction kit (Qiagen). Tg mice lines were generated by injecting the purified DNA fragments into fertilized BCF1 (C57BL/6 × C3H) oocytes. The incorporation of the transgene was confirmed by PCR analysis using DNA extracted from the tail and a set of primers to amplify a fragment encompassing the calmegin promoter and the MOR23-encoding gene. The breeding lines of mice were maintained by backcrossing C57BL/6CrSlc.

Imaging of intracellular Ca^{2+} levels

Imaging of intracellular Ca^{2+} levels in HEK293 cells co-expressing Flag/rhodopsin-tagged MOR23 and $G\alpha_{15}$ was performed as described previously (Kajiya et al., 2001; Katada et al., 2003). Briefly, 60-70% confluent HEK293 cells were transfected with 2.0 μg pME-18S-tagged MOR23 and 1.5 μg pME-18S-Gα15 using Lipofectamine 2000 (Invitrogen). 24 hours after transfection, cells were loaded with 5 μM fura-2/AM (Molecular Probes) for 30 minutes at 37°C and subjected to Ca^{2+} imaging assay.

For imaging of Ca^{2+} levels in spermatogenic cells, seminiferous tubules were isolated from mouse testis in PBS. Several pieces of seminiferous tubules were treated for 7-10 minutes with 0.05% trypsin, for 5 minutes with 0.025% trypsin inhibitor (Sigma) and finally for 10 minutes with 0.12 U μl^{-1} DNase I (Sigma). The trypsin-treated tubules were washed with HS buffer (135 mM NaCl, 5 mM KCl, 2 mM $CaCl_2$, 1 mM $MgCl_2$, 10 mM glucose, 10 mM lactic acid, 1 mM pyruvic acid, 30 mM HEPES, pH 7.4) supplemented with 15 mM $NaHCO_3$ and then spermatogenic cells were isolated on an uncoated glass-bottomed dish (Iwaki, Chiba, Japan) using an elastic glass pipette. The cells were loaded for 15 minutes at room temperature with 5 μM fura-2/AM and the dish was mounted in the recording chamber. Intracellular Ca^{2+} levels were monitored as the ratio of fura-2 fluorescence (at 510 nm) by excitation at 340 nm and 380 nm. Odorants were applied sequentially to the cells with a peristaltic pump at a flow rate of 1.5 ml $minute^{-1}$, and cells were continuously washed with HS buffer between stimulant applications. Application of K8.6 (135 mM KCl, 5 mM NaCl, 2 mM $CaCl_2$, 1 mM $MgCl_2$, 10 mM glucose, 10 mM lactic acid, 1 mM pyruvic acid, 30 mM HEPES, pH 8.6) (Wennemuth et al., 2000) was for 10 seconds.

For the imaging of sperm Ca^{2+} levels, spermatozoa were isolated from cauda epididymis and incubated for 15 minutes at 37°C in 500 μl HS buffer containing 15 mM $NaHCO_3$ and 5 mg ml^{-1} bovine serum albumin (BSA) (Sigma) to disperse the spermatozoa. The sperm suspension was then collected in a 1.5-ml plastic tube, and HS buffer was added to a final volume of 1 ml. The cells were incubated for 10 minutes at 37°C in an atmosphere of 5% CO_2/95% air. The upper 50-μl layer of the sperm suspension containing motile spermatozoa was transferred into a 1.5-ml tube, and 50 μl 10 μM fura-2 supplemented with 0.02% Cremophor/EL in HS buffer was added. The mixture was incubated for 30 minutes at 37°C, after which a 100-μl sample of the fura-2-loaded sperm suspension was placed on a laminin (Invitrogen)-coated glass-bottomed dish. After a few minutes, the medium on the dish was gently replaced with fura-2-free HS buffer and the dish was washed three times to remove unattached sperm and excess fura-2. Intracellular Ca^{2+} levels were measured for 10 minutes at 10-second intervals to reduce photobleaching of fura-2 and damage to sperm. Odorants were applied by adding 5 μl 50 mM solutions to the experimental dish containing 100 μl HS buffer. The final concentration of the stimulant was calculated assuming uniform distribution in the experimental medium.

Studies of sperm chemotaxis by tracking analysis

Spermatozoa were isolated from cauda epididymis into TYH buffer (120 mM NaCl, 5 mM KCl, 1.7 mM $CaCl_2$, 1.2 mM KH_2PO_4, 1.2 mM $MgSO_4$, 25 mM $NaHCO_3$, 1 mM pyruvic acid, 5.6 mM glucose, 5 mg ml^{-1} BSA) (Toyoda, 1971) supplemented with 30 mM HEPES and adjusted to pH 7.2 with NaOH as described for the preparation of sperm for Ca^{2+} imaging. The dispersed sperm suspension was collected in a 1.5-ml plastic tube, adjusted to 1×10^6-3×10^6 cells ml^{-1} and incubated for 20 minutes at 37°C in an atmosphere of 5% CO_2/95% air. Microcapillary tubes were loaded with 50-mM odorant, 10-mM 8-Br-cAMP or 10× K8.6, and the tube was placed on a Sigma Coat (Sigma)-coated glass-bottomed 3.5-mm dish (Iwaki) containing 300 μl of TYH buffer. Spermatozoa (30 μl 1×10^6-3×10^6 cells ml^{-1}) were applied gently at the edge of the dish and 1 cm away from the tip of the microcapillary tube, and 30 nl the stimulant was ejected from microcapillary tube using Digital Microdispenser (Drummond Scientific, USA) into the dish. The movement of spermatozoa toward the microcapillary tube was observed for 10 minutes using a DP-70 digital camera (Olympus) in a monitoring field of 0.8×0.6 mm. For sperm tracking analysis, the migration of each spermatozoon was traced manually at 1 second intervals during the time period 3-6 minutes after the ejection of the stimulant from the microcapillary. The traced spermatozoa were selected randomly but a trace that ended within 10 seconds was excluded from the analysis.

Sperm flagellar analysis

Sperm suspensions were prepared as described for the analysis of sperm chemotaxis. Sperm suspension (10 μl) was transferred to a 1.5-ml tube and mixed with 10 μl 2× stimulant solution. A 10-μl sample of the stimulated sperm suspension was mounted on a glass slide and fitted with 18×18 mm coverslips (Matsunami), and phase-contrast images were recorded with the DP70 digital camera. For Ca^{2+}-free assay, sperm were isolated from cauda epididymis and dispersed into Ca^{2+}-free buffer (120 mM NaCl, 6.7 mM KCl, 1.2 mM KH_2PO_4, 1.2 mM $MgSO_4$, 25 mM $NaHCO_3$, 1 mM pyruvic acid, 5.6 mM glucose, 5 mg ml^{-1} BSA, 30 mM HEPES) for 30 minutes. The sperm suspension was diluted fivefold in Ca^{2+}-free or Ca^{2+}-containing TYH buffer, and then added to equal volume of Ca^{2+}-free or TYH buffer containing 5 mM lyral. The sperm suspension, which contained more than 40% non-motile irregular sperm in buffer condition, was not used in this assay.

Results

Expression of MOR23 in testis

To clarify the function of MOR23 in germ cells, we first examined the expression of MOR23. Reverse-transcriptase PCR (RT-PCR) analysis showed that MOR23 is expressed in both the olfactory epithelium and the testis, but not in the vomeronasal organ, ovary, brain or kidney (Fig. 1A). We next examined the expression of MOR23 during the stages of spermatogenic development in C57BL/6 adult mouse testis by in situ hybridization using the TSA biotin system. Hybridization signals for the MOR23 antisense probe were detected in the adluminal cells of ~30% of the seminiferous tubules (Fig. 1B). Identical patterns were obtained using AP-conjugated (Fig. 1B) and HRP-conjugated (Fig. 1D) streptavidin. No signal was obtained using a MOR23 sense probe (Fig. 1C), indicating that staining with the antisense probe was specific for MOR23-encoding mRNA. In addition, very faint signals were observed when the TSA system was not used, suggesting that MOR23-encoding transcripts are

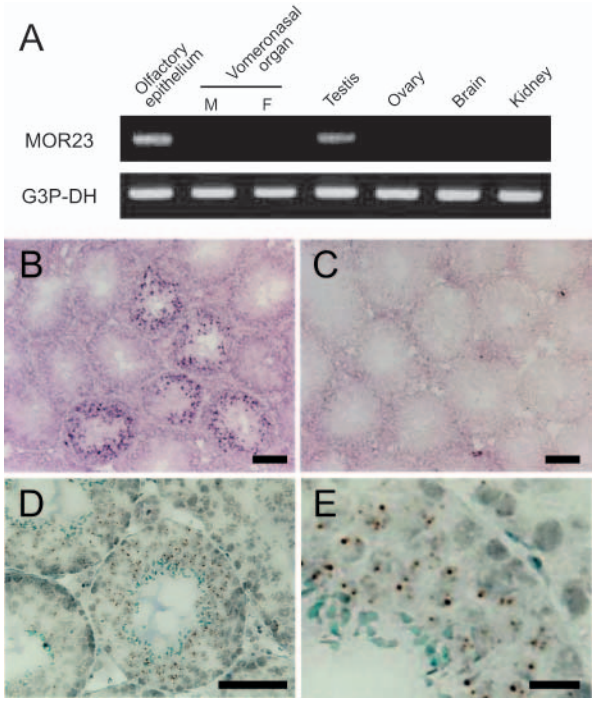

Fig. 1. Expression and localization of MOR23-encoding transcripts in mouse testis. (A) Tissue distribution of MOR23-encoding transcripts. Expression of MOR23 was assessed by RT-PCR. F, female; G3P-DH, glyceraldehyde-3-phosphate dehydrogenase; M, male. (B-E) The distribution pattern of the MOR23-encoding transcript was analysed by in situ hybridization. (B,D) Detection of MOR23-encoding mRNA with an antisense probe. MOR23-encoding mRNA was detected in a few seminiferous tubules using a TSA biotin system with AP- or HRP-conjugated streptavidin. (C) Control for nonspecific staining using a MOR23 sense probe; no signal was observed. (E) A high-magnification image of the MOR23 antisense probe staining indicates that the MOR23-encoding transcript is localized in spermatogenic cells. Hybridization signals detected with AP-streptavidin followed by NBT/BCIP are stained purple (B,C), whereas those detected with HRP-streptavidin followed by DAB are stained brown and nuclei are counterstained with methyl green (D,E). Scale bars, 100 μm (B-D), 20 μm (E).

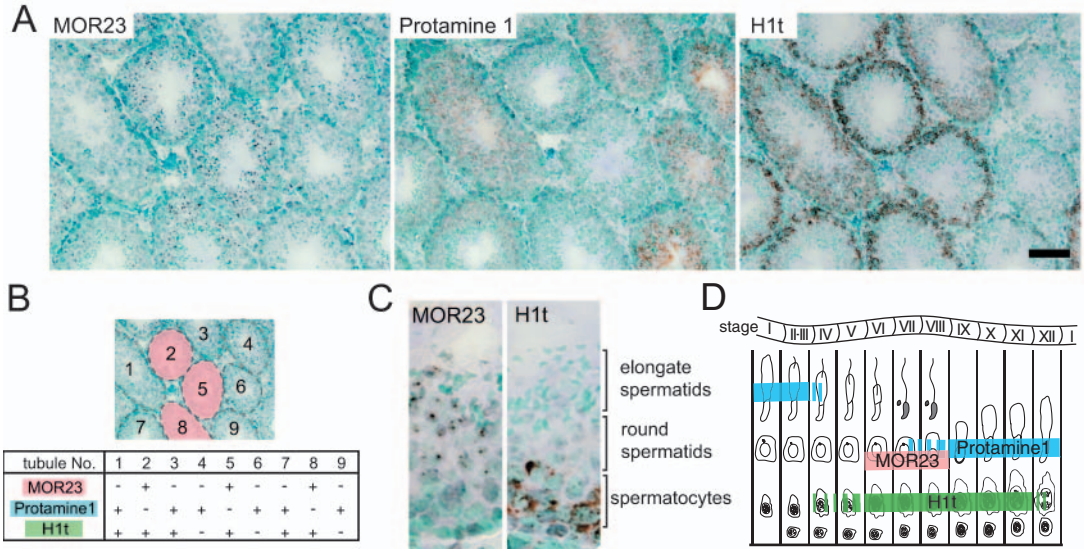

Fig. 2. Developmental expression pattern of MOR23 in mouse testis. (A) In situ hybridization using protamine 1 or H1t antisense probe was performed in serial sections to determine the stages of the seminiferous tubes expressing MOR23. (B) Individual tubules are numbered in the image, and the presence (+) or absence (–) of MOR23, protamine 1 and H1t in the corresponding tubules are shown in the table. MOR23-encoding transcripts were observed in seminiferous tubules from which protamine-1-encoding transcripts were absent but H1t transcripts were present. (C) Expression patterns of MOR23 and H1t in the corresponding areas of serial sections. MOR23-encoding transcripts are localized in the round spermatid layer, whereas H1t-encoding mRNA was found in spermatocytes. (D) Diagram of the 12-stage growth cycle of mouse spermatogenesis (Russell, 1990) showing the stages expressing MOR23 (magenta), protamine 1 (blue) and H1t (green) transcripts. MOR23 was expressed during stages VI-VIII. Scale bar, 100 μm.

present at low levels in testicular cells. A magnified image (Fig. 1E) shows that MOR23-encoding mRNA is localized in spermatogenic cells, possibly within the chromatoid body that might participate in the storage and transport of germ-cell-specific gene products, including germ-cell-specific RNA-binding protein (Noce et al., 2001).

Different seminiferous tubules contained distinct groups of spermatogonia, spermatocytes, and spermatids at various points of development. To determine at which developmental stage MOR23 is expressed, we examined serial sections of seminiferous tubules for protamine 1 and H1t transcripts and also for their nuclear morphologies based on counterstaining with methyl green (Fig. 2A). According to the 12-stage sperm development cycle in mice (Russell, 1990), protamine 1 is expressed at stages I-III and IX-XII (Mali et al., 1989), whereas H1t is expressed at stages VI-XII (Drabent et al., 1996). MOR23 transcripts were observed in seminiferous tubules that expressed H1t but had little or no expression of protamine 1 (Fig. 2B). In the seminiferous tubules, MOR23 transcripts were localized to inner layer cells but not to the spermatocyte layer expressing H1t in the corresponding seminiferous tubule in the serial sections (Fig. 2C). These results suggest that MOR23 is transcribed in round spermatids during stages VI-VIII of sperm development (Fig. 2D).

Effects of odorants on intracellular Ca^{2+} in MOR23-expressing HEK293 cells

MOR23 recognizes the floral odorant lyral and mediates an increase in intracellular Ca^{2+} in olfactory neurons (Touhara et al., 1999). To investigate this further, we analysed the effect of lyral on the level of intracellular Ca^{2+} in HEK293 cells transiently co-expressing Flag/rhodopsin-tagged MOR23 and the promiscuous G protein $G\alpha_{15}$. Intracellular Ca^{2+} levels were assessed using the Ca^{2+}-sensitive dye fura-2. We found that MOR23-expressing HEK293 cells responded to lyral in a dose-dependent manner (Fig. 3B). Treatment with 3 mM lyral caused an increase in Ca^{2+} in 38±8.6% of the cells (average from three experiments) and the average amplitude was a change in fluorescence ratio (ΔF) of 0.18±0.03 (average from ten cells in three experiments). In addition, bourgeonal, which has been reported to cause chemotaxis in human sperm (Spehr et al., 2003), had no effect on the level of intracellular Ca^{2+}. Likewise, heptanal, which is a ligand for the mouse I7 receptor (Araneda et al., 2000; Zhao et al., 1998) and is also expressed in testis (data not shown), did not enhance the level of intracellular Ca^{2+} (Fig. 3). These results suggest that bourgeonal and heptanal are not ligands for MOR23 and confirm the specific effect of lyral on MOR23.

Effects of odorants on intracellular Ca^{2+} in spermatids and spermatozoa

We next examined the effect of odorants on the level of intracellular Ca^{2+} in spermatogenic cells isolated from C57BL/6 mouse testis. Similar to the observations in the HEK293 cells, lyral induced a dose-dependent increase in intracellular Ca^{2+} as indicated by an increase in ΔF ratio (Fig. 4A). The threshold concentration for a response to lyral in spermatogenic cells was slightly higher than that in the MOR23-transfected HEK293 cells (i.e. HEK 293 cells, ~0.3 mM; spermatids, ~1 mM). As a positive control for Ca^{2+}-response (including cell viability, Ca^{2+}-sensitive dye loading and stable adhesion to glass-base dish), we also stimulated

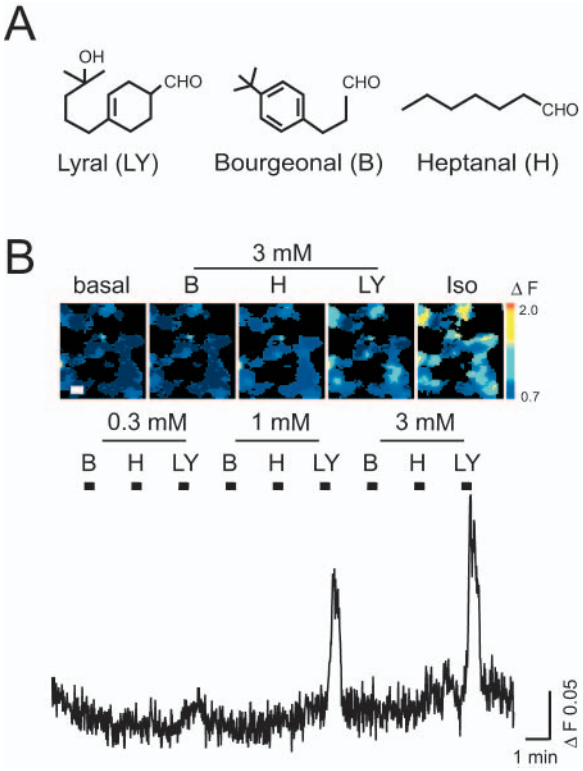

Fig. 3. Effect of lyral on Ca^{2+} levels in HEK293 cells expressing MOR23. (A) Chemical structures of odorants used in this study. (B) Effect of various treatments on Ca^{2+} levels. (top) Pseudocolored images of fura-2-loaded HEK293 cells stimulated with 3 mM odorant or isoproterenol (Iso). Iso, which causes Ca^{2+} increase in HEK293 cells via intrinsic β-adrenergic receptors and transfected Gα15, was used as a control for Gα15 co-transfection. Scale bar, 20 μm. (bottom) The Ca^{2+} response profile of MOR23-expressing HEK293 cells. Odorants were applied for 15 seconds during the time indicated by the bars, and cells were continuously washed with buffer between stimulant applications. B, bourgenonal; H, heptanal; LY, lyral.

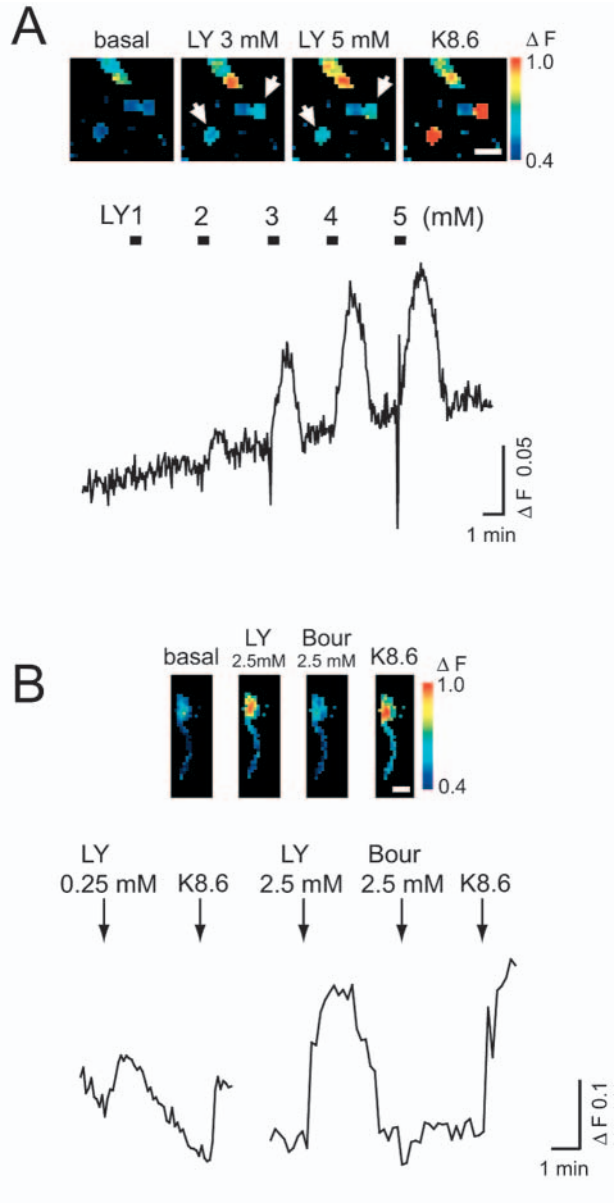

Fig. 4. Effect of lyral on Ca^{2+} levels in spermatogenic cells and spermatozoa. (A) Pseudocolored image and representative trace of Ca^{2+} levels in spermatogenic cells. Different concentrations of lyral were applied for 15 seconds during the times indicated by the bars and cells were continuously washed with buffer between stimulant applications. K8.6, a high potassium solution, was used as a positive control for cell viability. (top) Pseudocolored images of the Ca^{2+} levels. The cells indicated with white arrows display dose-dependent effects of lyral (scale bar, 20 μm). (bottom) Recordings of the change in fluorescence from single spermatogenic cell. (B) Pseudocolored image and representative trace of Ca^{2+} levels in cauda epididymal sperm. The response profile shows the change of ΔF ratio calculated in the entire area of the responding sperm head. Arrows indicate the application of an odorant or K8.6. Lyral (LY) but not bourgeonal (Bour) increased the level of Ca^{2+} in epididymal sperm. Scale bar, 4 μm.

them with K8.6, a high potassium solution that induces an increase in intracellular Ca^{2+} in living spermatogenic cells and spermatozoa (Wennemuth et al., 2000). In all Ca^{2+}-imaging experiments, the proportion of lyral-responding cells was calculated based on K8.6-responding population that was ~60% of total prepared cells. Stimulation with 3 mM lyral caused an increase in intracellular Ca^{2+} in 29±7.2% of the K8.6-responding spermatogenic cells (142 out of 513 cells in 18 preparations). This is a reasonable number, considering that in situ hybridization showed that MOR23 transcripts occur in the round spermatids of approximately 30% of the seminiferous tubules (Fig. 1B).

Stimulation with lyral also caused an increase in intracellular Ca^{2+} in cauda epididymal sperm. The Ca^{2+}-response to lyral was observed as low as 250 μM lyral stimulation (three out of 34 in five preparations), and the proportion responding epididymal spermatozoa to 2.5 mM lyral was 11±3.5% (11 out of 107 K8.6-responding spermatozoa from six preparations) (Fig. 4B). Treatment with 2.5 mM dihydromyrcenol, a compound that is structurally similar to lyral but is not a ligand for MOR23 (Touhara et al., 1999), did not cause an increase in intracellular Ca^{2+} (data not shown). The order of odorant application did not affect the changes in intracellular Ca^{2+} (data not shown). These results suggest that a lyral receptor,

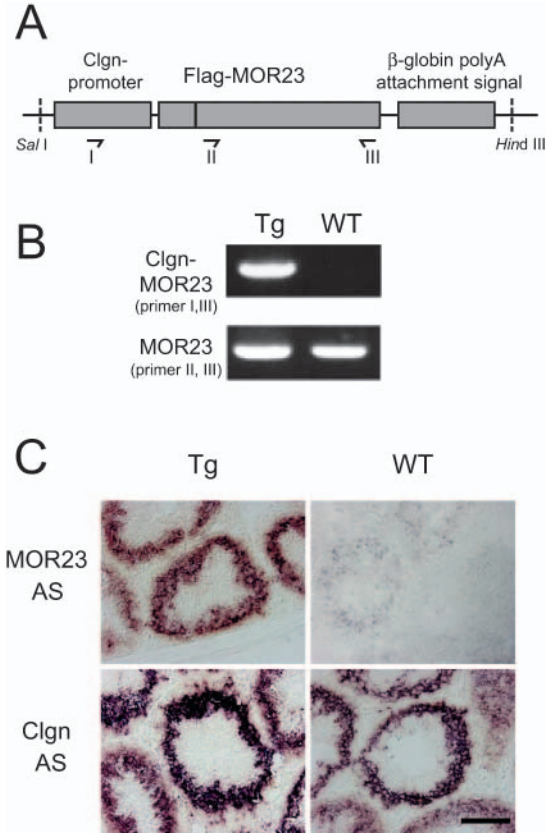

Fig. 5. Construction of transgenic (Tg) mice expressing MOR23 in the testis under the control of the calmegin promoter. (A) The transgene used to generate the Tg mouse line. The arrows show the primers used for genome PCR analysis. (B) Genome PCR analysis with primer pairs I and III demonstrate the insertion of transgene. PCR products with primer pairs II and III were derived from endogenous MOR23. (C) In situ hybridization using DIG-labeled antisense MOR23 probe (MOR23 AS) revealed high-level expression of the MOR23 transgene in Tg mouse testis. Hybridization signals were detected without the TSA system. Calmegin antisense probe (Clgn AS) was used as a positive control. WT, wild-type mouse. Scale bar, 100 μm.

potentially MOR23, is functionally expressed in a proportion of spermatids and spermatozoa. Finally, unlike human sperm (Spehr et al., 2003), none of the 76 mouse spermatozoa tested responded to bourgeonal (Fig. 4B). This finding is consistent with the recent unpublished observation that bourgeonal did not induce Ca^{2+} increases in mouse sperm (Spehr et al., 2004).

Generation of mice expressing a MOR23-encoding transgene in testis

To confirm that the effect of lyral on germ cells is mediated by MOR23, we generated Tg mice expressing high levels of MOR23 in all spermatids. To direct expression of MOR23 in the testis, we linked MOR23 to the promoter for calmegin, a chaperone expressed in the testis (Watanabe et al., 1995) (Fig. 5A). Genome PCR analysis with specific primers confirmed that MOR23-encoding transgene was incorporated in the Tg mice (Fig. 5B). In situ hybridization further revealed that expression of the MOR23-encoding transgene in the testis of three different Tg mouse lines was much higher than the expression of the endogenous MOR23-encoding gene in wild-type mouse testis (Fig. 5C). The expression pattern of the MOR23-encoding transgene in Tg mouse testis was identical to that of calmegin transcripts observed from late pachytene spermatocyte stage to elongated spermatid stage (Watanabe et al., 1994). Finally, using immunoprecipitation and western-blot analysis with an anti-Flag antibody, we found Tg-mouse-specific proteins in the lysates of testis and epididymis, confirming expression of the Flag-MOR23 protein (data not shown).

Response of germ cells in MOR23 Tg mice to lyral

We next examined the responsiveness of germ cells from MOR23 Tg mice to lyral. We compared the proportion of responding cells as well as the amplitude of the responses for Tg and wild-type mice. The threshold concentration for stimulation by lyral in spermatogenic cells from Tg mice was similar to that in cells from wild-type mice (approximately 1 mM) (Fig. 6A, left). The average amplitude of maximal increases in fura-2 fluorescence in spermatogenic cells from Tg mice (ΔF ratio=0.16±0.01 for 16 cells from three preparations) was higher than that in spermatogenic cells from wild-type mice (0.09±0.01 for 16 cells from three preparations) (Fig. 6A, middle). In addition, the proportion of Tg spermatogenic cells responding to 3 mM lyral was 60±8.3% (304 out of 533 spermatogenic cells from 19 preparations), whereas it was 29±7.2% in spermatogenic cells from wild-type mice (142 out of 513 spermatogenic cells from 18 preparations) (Fig. 6A, right). The increase in the number of responsive cells in Tg mice compared with wild-type mice was probably due to the expression of MOR23 at earlier stages of spermatogenesis under the control of the calmegin promoter.

We also examined the effect of lyral on sperm. As in the case of spermatogenic cells, we found that lyral elicited intracellular Ca^{2+} increases in Tg mouse sperm (Fig. 6B, left). The proportion of spermatozoa from Tg mice responding to 2.5 mM lyral was 53±14% (39 out of 76 sperm from five preparations), whereas the proportion in spermatozoa from wild-type mice was 11±3.5% (11 out of 107 sperm from six preparations) (Fig. 6B, middle). These results suggest that about half of the spermatozoa have the potential to express MOR23, though only a proportion of spermatozoa appear to express MOR23 in wild-type mice. By contrast, the amplitude of changes induced by lyral was not significantly different than in spermatozoa from wild-type mice (Fig. 6B, right), indicating that the level of endogenous MOR23 expression in spermatozoa was high enough to give a maximal response to lyral. These results suggest that MOR23 functions as a lyral receptor in spermatozoa and support the idea that lyral induces an increase in intracellular Ca^{2+} in spermatozoa through MOR23. Bourgeonal did not cause an increase in intracellular Ca^{2+} in Tg mouse sperm (0 out of 31 sperm in nine experiments, data not shown), further supporting our finding that MOR23 and any other ORs expressed on mouse spermatozoa do not recognize bourgeonal.

Effect of lyral on sperm movement in a sperm accumulation assay

Because many studies have demonstrated that intracellular

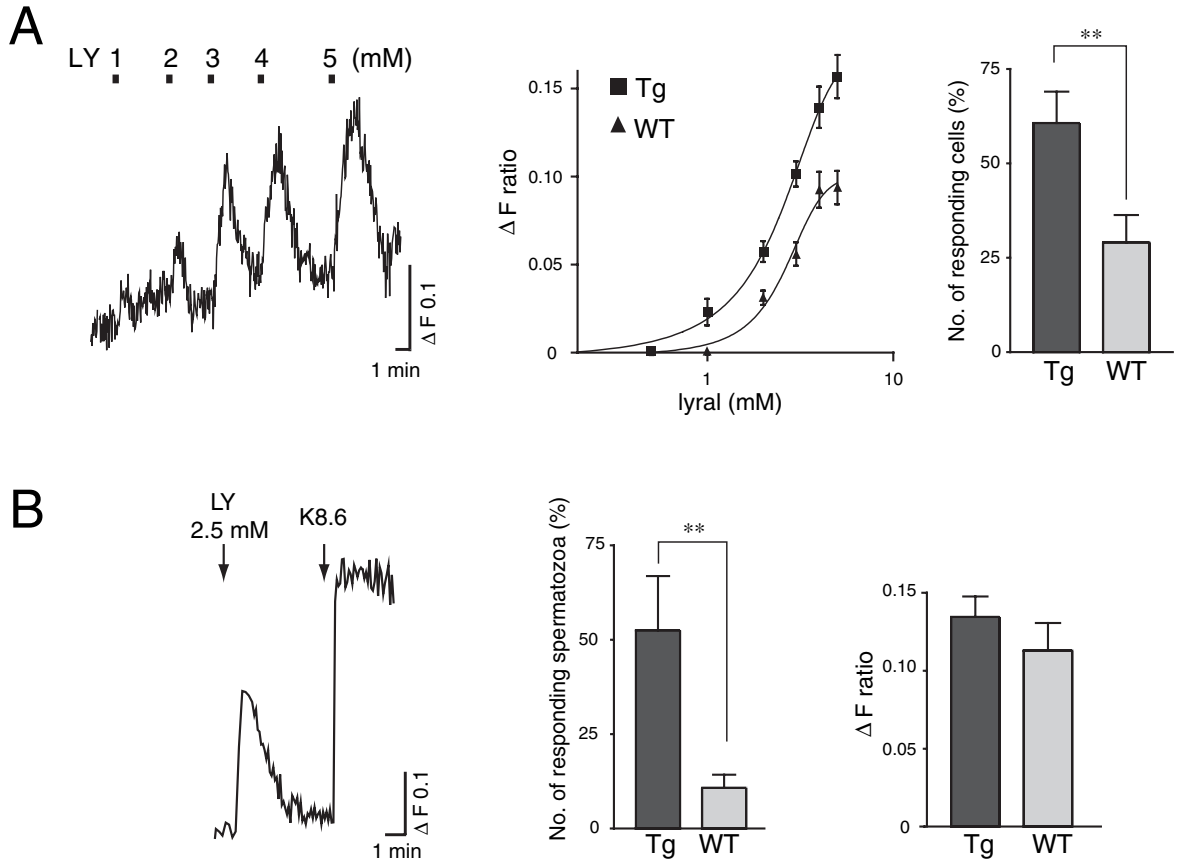

Fig. 6. Effect of lyral on Ca^{2+} levels in spermatogenic cells and cauda epididymal sperm from MOR23 Tg and wild-type mice. (A) (left) A representative response of Tg mouse testis spermatogenic cells to increasing concentrations of lyral. (middle) A dose-response curve for lyral in spermatogenic cells from Tg (filled squares) and wild-type (filled triangles) mouse testis (± s.e., n=3). (right) The proportion of spermatogenic cells responding to 3 mM lyral in Tg and wild-type mice. **, P<0.01 (Student's t test, ± s.e., n=18). (B) (left) A representative response of an epididymal spermatozoon isolated from a Tg mouse to lyral and K8.6. (middle) Proportion of spermatozoa from Tg and wild-type mice that respond to 2.5 mM lyral. **, P<0.01 (Student's t test, ± s.e., n=6). (right) The average amplitude of the response to 2.5 mM lyral in Tg and wild-type mouse sperm. LY, lyral; WT, wild type.

Ca^{2+} regulates sperm motility (Eisenbach, 1999; Suarez and Ho, 2003), we next examined the physiological relevance of MOR23-mediated increases in intracellular Ca^{2+} to sperm movement. Spermatozoa from Tg mice (30 μl of 10^6 spermatozoa ml^{-1}) were placed at the edge of a 3.5-cm glass-bottomed dish containing 0.3 ml buffer, approximately 1 cm from the tip of a microcapillary containing buffer or 50 mM lyral. A gradient was generated by ejecting 30 nl of the solution from the microcapillary, and the movement of spermatozoa around the tip of the microcapillary glass was monitored for 10 minutes with a digital camera. A significant amount of spermatozoa accumulated around the tip of the microcapillary glass from which lyral was ejected, whereas spermatozoa did not reach or remain around the microcapillary containing TYH buffer (Fig. 7A).

Fig. 7B shows the time course of the accumulation of Tg spermatozoa in a 200-μm radius circle around the tip of the microcapillary. When lyral was ejected from the microcapillary, some spermatozoa began to arrive and stayed in the observation area within 3-5 minutes. By contrast, TYH buffer had little effect on sperm accumulation. A significant difference between lyral and TYH buffer was observed after 4 minutes (P<0.01 after 4-7 minutes; P<0.05 after 8-10 minutes). Similarly, a significant amount of wild-type spermatozoa accumulated around the microcapillary tip when lyral was ejected, although it was less than for Tg mouse sperm (Fig. 7C). Significant sperm accumulation was not observed when the microcapillary contained dihydromyrcenol or bourgeonal (Fig. 7C), indicating that the sperm accumulation was specifically due to lyral and not the result of a non-specific chemical effect of lyral. Furthermore, K8.6 and 8-Br-cAMP, which induce Ca^{2+} influx in spermatozoa, did not cause the accumulation of spermatozoa, suggesting that OR-mediated Ca^{2+} influx is necessary for inducing the accumulation (Fig. 7C).

Examination of sperm movement by tracking analysis

Sperm accumulation could result from chemotaxis, chemokinesis or trapping. To determine which of these mechanisms accounted for sperm accumulation to lyral, we performed tracking analysis, which can distinguish between chemotaxis and other mechanisms that can cause sperm accumulation (Eisenbach and Tur-Kaspa, 1999; Jaiswal et al., 1999; Ralt et al., 1994). Tracking analysis was carried out on wild-type spermatozoa that appeared in the monitoring field.

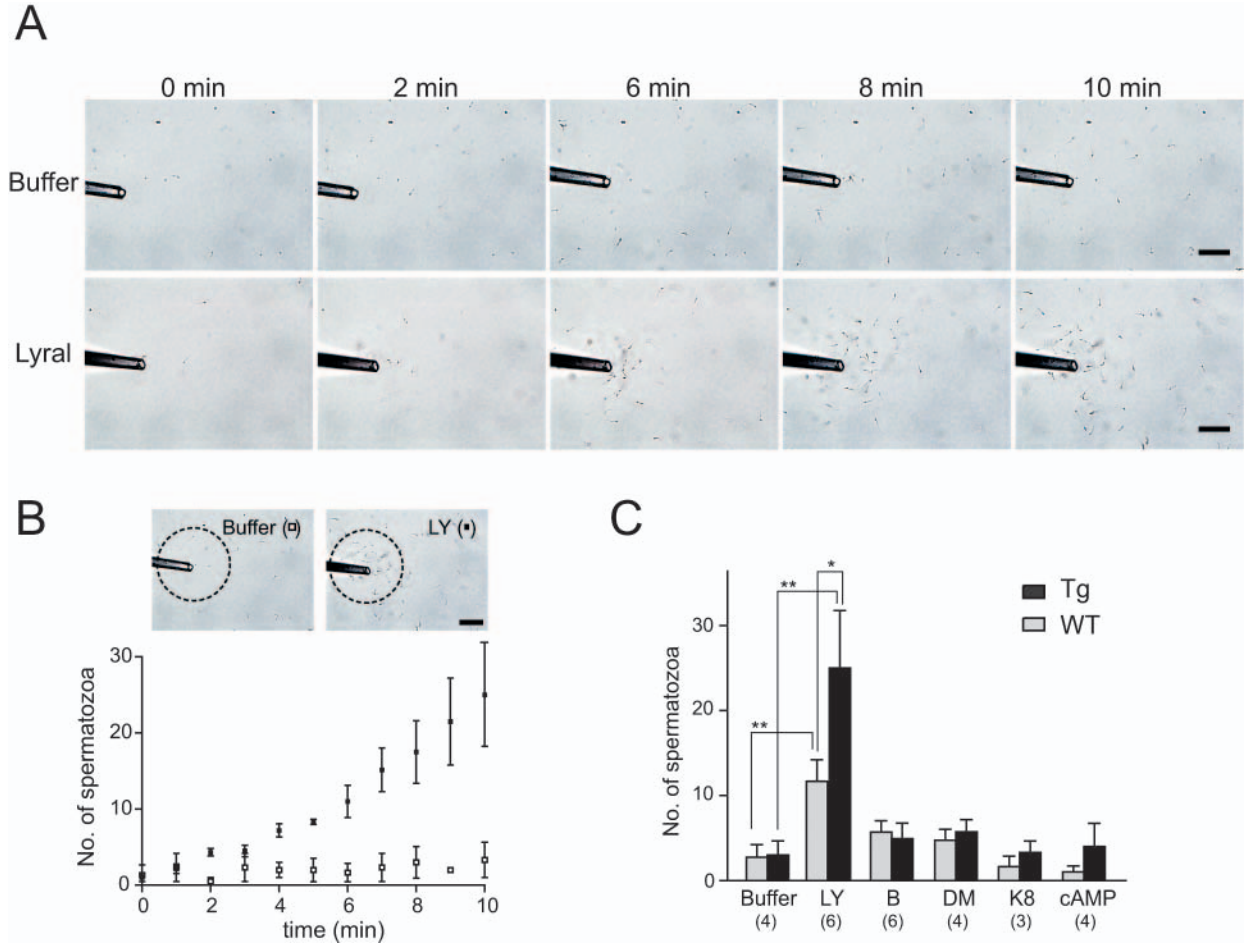

Fig. 7. Effect of gradients of various stimulants on sperm accumulation. (A) Representative images of mouse spermatozoa from Tg mice showing sperm accumulation around the tip of a glass microcapillary containing 50 mM lyral or buffer. Scale bar, 100 μm. (B) Time course of spermatozoa accumulation in a 200-μm radius circular area around the tip of the microcapillary. Images are representative of six independent experiments for lyral and three for buffer. The graph shows the average numbers of sperm within the accumulation area as a function of time after the ejection of lyral (filled squares) or buffer (empty squares) (± s.e.; buffer, n=4; LY, n=6). A significant difference was observed between lyral and buffer after 4-7 (P<0.01) and 8-10 (P<0.05) minutes. (C) The numbers of Tg and wild-type spermatozoa attracted toward gradients of buffer, 50 mM lyral (LY), 50 mM dihydromyrcenol (DM), 50 mM bourgeonal (B), 10× concentrated K8.6 (K8) or 10-mM 8-Br-cAMP (cAMP). The graph shows the number of spermatozoa that accumulated in the 200-μm radius circle around the tip of each microcapillary. The numbers in parentheses represent the number of experiments performed for each reagent. *, P<0.05; **, P<0.01 (Student's t test, ± s.e.).

The migration of each spermatozoon was traced manually at intervals of 1 second during the 3-6 minute after the ejection of lyral or TYH buffer from the microcapillary (Fig. 8A). The proportion of spermatozoa in the monitoring field that swam toward the microcapillary was 44.5±0.5% for lyral (22 out of 49 traced spermatozoa in four experiments) and 24.5±7.4% for TYH buffer (nine out of 42 traced spermatozoa in four experiments). Among 22 spermatozoa that reached the lyral-containing microcapillary, 18 (80%) made directional changes towards the lyral gradient, whereas spermatozoa did not make directional changes towards a capillary containing TYH buffer. These results suggest that lyral-mediated sperm accumulation is due to chemotaxis.

Analysis of sperm flagella

In rat sperm, an increase in intracellular Ca^{2+} enhances flagellar beating asymmetry, whereas a high concentration of intracellular Ca^{2+} induces quiescence coupled with a distinct fishhook-like configuration owing to maximal asymmetry (Gibbons and Gibbons, 1980; Lindemann and Goltz, 1988). Similarly, during the course of our sperm accumulation assay, we observed a decrease in progressive motility of spermatozoa near the lyral-containing microcapillary tip as well as a curvature of flagella in an opposite direction. When spermatozoa were exposed to 2.5 mM lyral, the movement arrest with fishhook-like flagellar configuration was induced in 19.2±1.0% of wild-type spermatozoa (63 out of 323 from five experiments) (Fig. 8B). The arrest with the flagellar curvature was not observed with bourgenonal, dihydromyrcenol or buffer control, although sperm movement was arrested with straight flagellar configuration at high concentrations of bourgenonal or dihydromyrcenol (2.5 mM). The movement suppression induced by these odorants was probably due to a nonspecific chemical damage, which might explain why some sperm accumulated near the capillary containing these chemicals

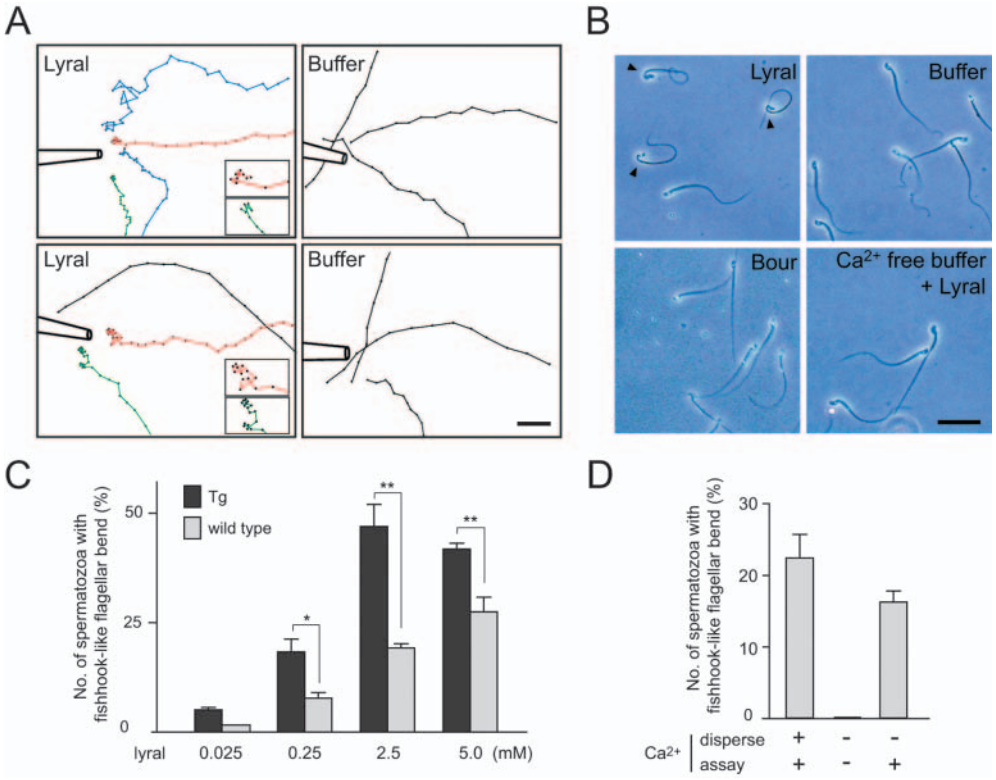

Fig. 8. Tracking analysis of the movement of mouse spermatozoa towards a gradient of lyral and analysis of flagellar configuration. (A) A representative trace of wild-type spermatozoa towards a capillary containing 50 mM lyral or buffer. Traces were made from the sperm accumulation assay at 1 second intervals 3-6 minutes after the ejection of the stimulant. Traces exhibiting directional changes are colored. Insets show an enlargement of the red and green traces. Scale bar, 100 μm. (B) Effect of lyral on flagellar configuration. Representative images of the flagellar shape of wild-type mouse spermatozoa exposed to 2.5 mM lyral, 2.5 mM bourgeonal (Bour) or buffer. Arrested spermatozoa with fishhook-shaped flagella (arrowheads) were found in lyral, whereas this configuration was not observed in other odorants or in Ca^{2+}-free buffer containing 2.5 mM lyral. Scale bar, 50 μm. (C) The numbers of spermatozoa with fishhook-like flagellar configuration at various concentrations of lyral (*, $P<0.05$, **, $P<0.01$, Student's t test, ± s.e.; 25 μM, $n=3$; 0.25-5.0 mM, $n=4$). The effect of lyral on flagellar configuration was dose dependent. (D) Effects of extracellular Ca^{2+} on a lyral-mediated flagellar configurational change. Wild-type spermatozoa were dispersed in Ca^{2+}-free or Ca^{2+}-containing buffer (disperse – or +, respectively). The dispersed sperm were diluted in Ca^{2+}-free or Ca^{2+}-containing buffer (assay – or +, respectively) and then stimulated with 2.5 mM lyral (± s.e., $n=3$).

(Fig. 7C). The number of the fishhook-like flagellar sperm induced by lyral stimulation increased in a dose-dependent manner and was larger in Tg mice than that in wild-type mice (for 2.5 mM lyral, Tg mice had 47.0±5.0% fishhook-like flagellar sperm, whereas the wild type had 19.2±1.0%; from five experiments) (Fig. 8C). Furthermore, no fishhook-like flagellar configuration was induced by 2.5 mM lyral in spermatozoa in Ca^{2+}-free buffer, whereas flagellar curvature was observed again when the spermatozoa were returned into Ca^{2+}-containing buffer (Fig. 8D). These results support the idea that lyral stimulation of MOR23 causes an increase in intracellular Ca^{2+} and modulates flagellar configuration. Finally, the fishhook configuration was not observed with 1× K8.6 solution or 3 mM cAMP analog (data not shown), suggesting that a simple Ca^{2+} influx was not sufficient to cause sperm flagellar curvature.

Discussion

In this study, we investigated the functional consequence of MOR23 expression in mouse germ cells by using lyral, a cognate ligand of MOR23. Lyral caused an increase in intracellular Ca^{2+} in a proportion of spermatids and spermatozoa. Comparison of the responsiveness of MOR23 Tg and wild-type germ cells suggested that lyral increases intracellular Ca^{2+} via MOR23. A gradient of lyral appears to induce sperm accumulation by promoting changes in sperm flagellar asymmetry. These results imply that odorant-OR interaction causes intracellular Ca^{2+} increase and mediates the chemosensing ability of the spermatozoa.

During spermatogenesis, MOR23 appears to be expressed at specific stages in the round spermatids of approximately 30% of the seminiferous tubules. This expression during limited stages of spermatids is similar to the expression pattern of some members of the spermatid chemoreceptor family (a family of rat ORs) in the testis (Walensky et al., 1998). This contrasts with the report by Tatsura et al. (Tatsura et al., 2001) that TOR9, an OR family member, is expressed in 90% of seminiferous tubules. The large difference between the expression patterns could be attributed to differences between OR genes or to differences in hybridization conditions. We also observed that some other ORs distinct from MOR23 are expressed during earlier spermatogenic stages (data not shown), suggesting that there are at least two types of OR gene expression pattern during spermatogenesis. Further analysis of the expression patterns of other testicular ORs and generation of a reliable anti-OR antibody will be necessary to elucidate the functional consequence of different expression profiles of testicular ORs.

Imaging of intracellular Ca^{2+} with fura-2 showed that approximately 10% of cauda epididymal sperm responded to lyral, suggesting that MOR23 was expressed in a limited proportion of the total spermatozoa. A previous report demonstrated that approximately 5% of spermatozoa from dog testes are strongly stained with an antibody against DTMT, a dog OR (Vanderhaeghen et al., 1993). In addition, bourgeonal

induces an increase in intracellular Ca^{2+} in 36% of human sperm (Spehr et al., 2003). It therefore appears that each OR is expressed in 5-40% of the total sperm cells, depending on the OR and the species. Lyral caused an increase in intracellular Ca^{2+} in approximately 50% of spermatozoa in MOR23 Tg mice, suggesting that about half of the population of spermatozoa have the potential to respond to small molecules via ORs. Whether each sperm expresses one or multiple ORs remains unknown, and differences between the type of ORs expressed in individual sperm cells could provide heterogeneity related to an intergametic selection phenomenon. In this regard, only a limited proportion of spermatozoa exhibit chemotactic behavior in mammalian sperm chemotaxis assays. For example, only 13% of mouse sperm cells (Oliveira et al., 1999) and 2-12% of human sperm cells (Cohen-Dayag et al., 1994) show chemotaxis to follicular fluid. We also found that limited proportion of the mouse sperm accumulated towards an ascending gradient of lyral. Although it has been suggested that the number of chemoattracted sperm to follicular fluid corresponds to the population of capacitated sperm (Cohen-Dayag et al., 1995), our data suggest that the population of chemotactically active sperm are not likely to be restricted by capacitation, because the number of accumulated spermatozoa towards lyral was larger in Tg mice than in wild-type mice under the same capacitation conditions. It is, however, also possible that ORs are involved in capacitation and therefore that the population of capacitated sperm is higher in Tg mouse spermatozoa. It remains to be elucidated whether chemotaxis is regulated by capacitation or OR expression, or both.

Investigation of the chemotactic response to lyral by tracking analysis suggested that mouse sperm swam towards a gradient of lyral with directional changes, which are caused by Ca^{2+}-induced flagellar beating asymmetry. The sperm that reached the vicinity of the microcapillary tip appeared to arrest with a fishhook flagellar configuration associated with a high concentration of intracellular Ca^{2+}. The effects of intracellular Ca^{2+} on asymmetric flagellar changes are well documented in non-mammalian sperm and are thought to be essential for sperm chemotaxis (Eisenbach, 1999). Our study suggests that Ca^{2+}-mediated asymmetric flagellar changes are also involved in chemotaxis of mammalian sperm.

The Ca^{2+}-induced bend of sperm flagella has been reported to be the result of a local mechanism in which the mid-piece plays a crucial role (Gibbons and Gibbons, 1980; Lindemann and Goltz, 1988). We demonstrated that K8.6 and 8-Br-cAMP, which enhance intracellular Ca^{2+} in spermatozoa, did not cause sperm accumulation or sperm flagellar asymmetry. Thus, our results suggest that a simple Ca^{2+} influx alone is not sufficient to cause sperm chemotaxis. Rather, a local increase in Ca^{2+}, probably in the mid-piece, where ORs might be located as demonstrated for a dog testicular OR (Vanderhaeghen et al., 1993), is probably necessary for chemosensing and regulation of sperm motility.

ORs are known to recognize a range of structurally related odorants with various thresholds (Araneda et al., 2000; Kajiya et al., 2001). Although the threshold concentration for a MOR23 response to lyral is relatively high [i.e. 10-100 μM in olfactory neurons, ~300 μM in HEK293 cells (Fig. 3B), ~250 μM in germ cells (Fig. 4B, Fig. 8C)], endogenous MOR23 ligand(s) or other odorants might show higher affinity than lyral. The nature of possible endogenous ligand(s) for MOR23 is not currently known but it might be a small molecule, because many sperm chemoattractants are small chemicals or short peptides. For example, resact is a 14-amino-acid peptide that is released from the egg jelly layer and acts as a sperm chemoattractant in sea urchin (Ward et al., 1985). In addition, sperm-activating and -attracting factor, a chemoattractant for ascidian sperm, is a sulfated steroid (Yoshida et al., 1993), and the attractant for corals is an aliphatic alcohol with a molecular weight of 240 Da (Eisenbach, 1999). Thus, MOR23 probably recognizes a small ligand(s) that is structurally related to lyral and is released in the female reproductive tract. Interestingly, both bourgeonal and lyral are small organic compounds that possess an aldehyde group. Further work will focus on screening endogenous ligands to help understand the physiological role of ORs in sperm function.

In summary, our results suggest that the mouse testicular OR MOR23 functions as a chemosensor in sperm, and that MOR23-mediated increases in intracellular Ca^{2+} stimulate sperm motility. Several intriguing questions have remained to be elucidated. (1) Does each sperm express one or multiple ORs? (2) Is MOR23 the only OR that functions in mouse sperm? (3) What is the molecular mechanism of OR-mediated signaling in sperm? (4) Is there an endogenous ligand(s) for MOR23? (5) What is the functional relevance of MOR23 and an endogenous ligand for sperm-egg communication? The in situ hybridization technique for testicular OR genes and the MOR23-expressing Tg mouse lines established in this study are powerful tools with which to answer these questions. Identification of an endogenous OR ligand(s) possibly in the follicular fluid and its application to sperm-egg physiology will help to elucidate the basic developmental biology of cell motility and fertilization. Finally, we speculate that OR-mediated sperm-egg communication, which occurs after mating, is analogous to sex-pheromone-mediated tracking behavior observed in a wide range of species.

We thank F. Aoki, M. Kinukawa, S. Oda and H. Kataoka for valuable advice, Y. Nishimune for the calmegin promoter, T. Hasegawa Co. Ltd for odorants, and lab members for helpful discussion. This work was supported in part by grants from the Ministry of Education, Science, Sports, and Culture (MEXT) to K.T., K.Y. and M.O., and the Program for Promotion of Basic Research Activities for Innovative Biosciences (PROBRAIN) to K.T. K.T. is a recipient of grants from Uehara Memorial Foundation and Kato Memorial Bioscience Foundation.

References

Araneda, R. C., Kini, A. D. and Firestein, S. (2000). The molecular receptive range of an odorant receptor. *Nat. Neurosci.* **3**, 1248-1255.

Asai, H., Kasai, H., Matsuda, Y., Yamazaki, N., Nagawa, F., Sakano, H. and Tsuboi, A. (1996). Genomic structure and transcription of a murine odorant receptor gene: differential initiation of transcription in the olfactory and testicular cells. *Biochem. Biophys. Res. Commun.* **221**, 240-247.

Baldi, E., Luconi, M., Bonaccorsi, L. and Forti, G. (2002). Signal transduction pathways in human spermatozoa. *J. Reprod. Immunol.* **53**, 121-131.

Cohen-Dayag, A., Ralt, D., Tur-Kaspa, I., Manor, M., Makler, A., Dor, J., Mashiach, S. and Eisenbach, M. (1994). Sequential acquisition of chemotactic responsiveness by human spermatozoa. *Biol. Reprod.* **50**, 786-790.

Cohen-Dayag, A., Tur-Kaspa, I., Dor, J., Mashiach, S. and Eisenbach, M. (1995). Sperm capacitation in humans is transient and correlates with chemotactic responsiveness to follicular factors. *Proc. Natl. Acad. Sci. USA* **92**, 11039-11043.

Darszon, A., Beltran, C., Felix, R., Nishigaki, T. and Trevino, C. L. (2001). Ion transport in sperm signaling. *Dev. Biol.* **240**, 1-14.

Dawson, T. M., Arriza, J. L., Jaworsky, D. E., Borisy, F. F., Attramadal, H., Lefkowitz, R. J. and Ronnett, G. V. (1993). Beta-adrenergic receptor kinase-2 and beta-arrestin-2 as mediators of odorant-induced desensitization. *Science* **259**, 825-829.

Defer, N., Marinx, O., Poyard, M., Lienard, M. O., Jegou, B. and Hanoune, J. (1998). The olfactory adenylyl cyclase type 3 is expressed in male germ cells. *FEBS Lett.* **424**, 216-220.

Drabent, B., Bode, C., Bramlage, B. and Doenecke, D. (1996). Expression of the mouse testicular histone gene *H1t* during spermatogenesis. *Histochem. Cell Biol.* **106**, 247-251.

Eisenbach, M. (1999). Sperm chemotaxis. *Rev. Reprod.* **4**, 56-66.

Eisenbach, M. and Tur-Kaspa, I. (1999). Do human eggs attract spermatozoa? *BioEssays* **21**, 203-210.

Firestein, S. (2001). How the olfactory system makes sense of scents. *Nature* **413**, 211-218.

Gautier-Courteille, C., Salanova, M. and Conti, M. (1998). The olfactory adenylyl cyclase III is expressed in rat germ cells during spermiogenesis. *Endocrinology* **139**, 2588-2599.

Gibbons, B. H. and Gibbons, I. R. (1980). Calcium-induced quiescence in reactivated sea urchin sperm. *J. Cell Biol.* **84**, 13-27.

Izumi, H., Marian, T., Inaba, K., Oka, Y. and Morisawa, M. (1999). Membrane hyperpolarization by sperm-activating and -attracting factor increases cAMP level and activates sperm motility in the ascidian *Ciona intestinalis*. *Dev. Biol.* **213**, 246-256.

Jaiswal, B. S., Tur-Kaspa, I., Dor, J., Mashiach, S. and Eisenbach, M. (1999). Human sperm chemotaxis: is progesterone a chemoattractant? *Biol. Reprod.* **60**, 1314-1319.

Kajiya, K., Inaki, K., Tanaka, M., Haga, T., Kataoka, H. and Touhara, K. (2001). Molecular bases of odor discrimination: reconstitution of olfactory receptors that recognize overlapping sets of odorants. *J. Neurosci.* **21**, 6018-6025.

Katada, S., Nakagawa, T., Kataoka, H. and Touhara, K. (2003). Odorant response assays for a heterologously expressed olfactory receptor. *Biochem. Biophys. Res. Commun.* **305**, 964-969.

Kaupp, U. B., Solzin, J., Hildebrand, E., Brown, J. E., Helbig, A., Hagen, V., Beyermann, M., Pampaloni, F. and Weyand, I. (2003). The signal flow and motor response controling chemotaxis of sea urchin sperm. *Nat. Cell Biol.* **5**, 109-117.

Kirkman-Brown, J. C., Sutton, K. A. and Florman, H. M. (2003). How to attract a sperm. *Nat. Cell Biol.* **5**, 93-96.

Lindemann, C. B. and Goltz, J. S. (1988). Calcium regulation of flagellar curvature and swimming pattern in Triton X-100-extracted rat sperm. *Cell Motil. Cytoskeleton* **10**, 420-431.

Mali, P., Kaipia, A., Kangasniemi, M., Toppari, J., Sandberg, M., Hecht, N. B. and Parvinen, M. (1989). Stage-specific expression of nucleoprotein mRNAs during rat and mouse spermiogenesis. *Reprod. Fertil. Dev.* **1**, 369-382.

Malnic, B., Hirono, J., Sato, T. and Buck, L. B. (1999). Combinatorial receptor codes for odors. *Cell* **96**, 713-723.

Mombaerts, P. (1999). Seven-transmembrane proteins as odorant and chemosensory receptors. *Science* **286**, 707-711.

Noce, T., Okamoto-Ito, S. and Tsunekawa, N. (2001). Vasa homolog genes in mammalian germ cell development. *Cell Struct. Funct.* **26**, 131-136.

Oliveira, R. G., Tomasi, L., Rovasio, R. A. and Giojalas, L. C. (1999). Increased velocity and induction of chemotactic response in mouse spermatozoa by follicular and oviductal fluids. *J. Reprod. Fertil.* **115**, 23-27.

Parmentier, M., Libert, F., Schurmans, S., Schiffmann, S., Lefort, A., Eggerickx, D., Ledent, C., Mollereau, C., Gerard, C., Perret, J. et al. (1992). Expression of members of the putative olfactory receptor gene family in mammalian germ cells. *Nature* **355**, 453-455.

Ralt, D., Manor, M., Cohen-Dayag, A., Tur-Kaspa, I., Ben-Shlomo, I., Makler, A., Yuli, I., Dor, J., Blumberg, S., Mashiach, S. et al. (1994). Chemotaxis and chemokinesis of human spermatozoa to follicular factors. *Biol. Reprod.* **50**, 774-785.

Russell, L. D. (1990). *Histological and Histopathological Evaluation of the Testis*, pp. 119-161. Clearwater, FL: Cache River Press.

Spehr, M., Gisselmann, G., Poplawski, A., Riffell, J. A., Wetzel, C. H., Zimmer, R. K. and Hatt, H. (2003). Identification of a testicular odorant receptor mediating human sperm chemotaxis. *Science* **299**, 2054-2058.

Spehr, M., Schwane, K., Riffell, J. A., Barbour, J., Zimmer, R. K., Neuhaus, E. M. and Hatt, H. (2004). Particulate adenylate cyclase plays a key role in human sperm olfactory receptor-mediated chemotaxis. *J. Biol. Chem.* **279**, 40194-40203.

Suarez, S. S. and Ho, H. C. (2003). Hyperactivated motility in sperm. *Reprod. Domest. Anim.* **38**, 119-124.

Tatsura, H., Nagao, H., Tamada, A., Sasaki, S., Kohri, K. and Mori, K. (2001). Developing germ cells in mouse testis express pheromone receptors. *FEBS Lett.* **488**, 139-144.

Touhara, K. (2001). Functional cloning and reconstitution of vertebrate odorant receptors. *Life Sci.* **68**, 2199-2206.

Touhara, K. (2002). Odor discrimination by G protein-coupled olfactory receptors. *Microsc. Res. Tech.* **58**, 135-141.

Touhara, K., Sengoku, S., Inaki, K., Tsuboi, A., Hirono, J., Sato, T., Sakano, H. and Haga, T. (1999). Functional identification and reconstitution of an odorant receptor in single olfactory neurons. *Proc. Natl. Acad. Sci. USA* **96**, 4040-4045.

Toyoda, Y., Yokoyama, M. and Hoshi, T. (1971). Studies on the fertilization of mouse eggs in vitro. I. In vitro fertilization of eggs by fresh epididymal sperm. *Jpn. J. Anim. Reprod.* **16**, 147-151.

Vanderhaeghen, P., Schurmans, S., Vassart, G. and Parmentier, M. (1993). Olfactory receptors are displayed on dog mature sperm cells. *J. Cell Biol.* **123**, 1441-1452.

Vanderhaeghen, P., Schurmans, S., Vassart, G. and Parmentier, M. (1997). Specific repertoire of olfactory receptor genes in the male germ cells of several mammalian species. *Genomics* **39**, 239-246.

Walensky, L. D., Roskams, A. J., Lefkowitz, R. J., Snyder, S. H. and Ronnett, G. V. (1995). Odorant receptors and desensitization proteins colocalize in mammalian sperm. *Mol. Med.* **1**, 130-141.

Walensky, L. D., Ruat, M., Bakin, R. E., Blackshaw, S., Ronnett, G. V. and Snyder, S. H. (1998). Two novel odorant receptor families expressed in spermatids undergo 5′-splicing. *J. Biol. Chem.* **273**, 9378-9387.

Ward, G. E., Brokaw, C. J., Garbers, D. L. and Vacquier, V. D. (1985). Chemotaxis of *Arbacia punctulata* spermatozoa to resact, a peptide from the egg jelly layer. *J. Cell Biol.* **101**, 2324-2329.

Watanabe, D., Yamada, K., Nishina, Y., Tajima, Y., Koshimizu, U., Nagata, A. and Nishimune, Y. (1994). Molecular cloning of a novel Ca^{2+}-binding protein (calmegin) specifically expressed during male meiotic germ cell development. *J. Biol. Chem.* **269**, 7744-7749.

Watanabe, D., Okabe, M., Hamajima, N., Morita, T., Nishina, Y. and Nishimune, Y. (1995). Characterization of the testis-specific gene 'calmegin' promoter sequence and its activity defined by transgenic mouse experiments. *FEBS Lett.* **368**, 509-512.

Wennemuth, G., Westenbroek, R. E., Xu, T., Hille, B. and Babcock, D. F. (2000). CaV2.2 and CaV2.3 (N- and R-type) Ca^{2+} channels in depolarization-evoked entry of Ca^{2+} into mouse sperm. *J. Biol. Chem.* **275**, 21210-21217.

Weyand, I., Godde, M., Frings, S., Weiner, J., Muller, F., Altenhofen, W., Hatt, H. and Kaupp, U. B. (1994). Cloning and functional expression of a cyclic-nucleotide-gated channel from mammalian sperm. *Nature* **368**, 859-863.

Wiesner, B., Weiner, J., Middendorff, R., Hagen, V., Kaupp, U. B. and Weyand, I. (1998). Cyclic nucleotide-gated channels on the flagellum control Ca^{2+} entry into sperm. *J. Cell Biol.* **142**, 473-484.

Yoshida, M., Inaba, K. and Morisawa, M. (1993). Sperm chemotaxis during the process of fertilization in the ascidians *Ciona savignyi* and *Ciona intestinalis*. *Dev. Biol.* **157**, 497-506.

Yoshida, M., Murata, M., Inaba, K. and Morisawa, M. (2002). A chemoattractant for ascidian spermatozoa is a sulfated steroid. *Proc. Natl. Acad. Sci. USA* **99**, 14831-14836.

Zhang, X. and Firestein, S. (2002). The olfactory receptor gene superfamily of the mouse. *Nat. Neurosci.* **5**, 124-133.

Zhao, H., Ivic, L., Otaki, J. M., Hashimoto, M., Mikoshiba, K. and Firestein, S. (1998). Functional expression of a mammalian odorant receptor. *Science* **279**, 237-242.